



Published in final edited form as:

Nanomedicine. 2012 August ; 8(6): 793–803. doi:10.1016/j.nano.2011.11.003.

Bioactive silica based nanoparticles stimulate bone forming osteoblasts, suppress bone resorbing osteoclasts, and enhance bone mineral density *in vivo*

George R. Beck Jr., Ph.D.^{1,2,*}, Shin-Woo Ha, Ph.D.^{4,3}, Corinne E. Camalier, M.S.¹, Masayoshi Yamaguchi, Ph.D.¹, Yan Li, M.D.¹, Jin-Kyu Lee, Ph.D.⁴, and M. Neale Weitzmann, Ph.D.^{1,2,5,*}

¹The Division of Endocrinology, Metabolism and Lipids, Emory University School of Medicine, Atlanta GA 30322, USA

²The Winship Cancer Institute, Emory University School of Medicine, Atlanta GA 30322, USA

⁴The Department of Chemistry, Seoul National University, Seoul 151-747, Korea

⁵The Atlanta Department of Veterans Affairs Medical Center, Decatur, Georgia 30033, USA

Abstract

Bone is a dynamic tissue that undergoes renewal throughout life by a process whereby osteoclasts resorb worn bone and osteoblasts synthesize new bone. Imbalances in bone turnover lead to bone loss and development of osteoporosis and ultimately fracture, a debilitating condition with high morbidity and mortality. Silica is a ubiquitous biocontaminant that is considered to have high biocompatibility. We report that silica nanoparticles mediate potent inhibitory effects on osteoclasts and stimulatory effects on osteoblasts *in vitro*. The mechanism of bioactivity is a consequence of an intrinsic capacity to antagonize activation of NF- κ B, a signal transduction pathway required for osteoclastic bone resorption, but inhibitory to osteoblastic bone formation. We further demonstrate that silica nanoparticles promote a significant enhancement of bone mineral density (BMD) in mice *in vivo* providing a proof of principle for the potential application of silica nanoparticles as a pharmacological agent to enhance BMD and protect against bone fracture.

Keywords

Bone; Nanoparticle; Osteoclast; Osteoblast; Silica

Background

The skeleton is a highly dynamic organ that is regenerated throughout life by a process in which old bone is removed (resorbed) by osteoclasts and new bone synthesized by

© Published by Elsevier Inc.

*Corresponding Authors: M. Neale Weitzmann, Ph.D., 101 Woodruff Circle, 1305 WMRB, Atlanta, Georgia 30322-0001, Tel: (404) 727-1389, Fax (404) 727-1300, mweitzm@emory.edu; and George R. Beck, Ph.D., 101 Woodruff Circle, 1026 WMRB, Atlanta, Georgia 30322-0001, Tel: (404) 727-1340, Fax (404) 727-1300, george.beck@emory.edu.

³Shin-Woo Ha should be considered a joint first author.

Publisher's Disclaimer: This is a PDF file of an unedited manuscript that has been accepted for publication. As a service to our customers we are providing this early version of the manuscript. The manuscript will undergo copyediting, typesetting, and review of the resulting proof before it is published in its final citable form. Please note that during the production process errors may be discovered which could affect the content, and all legal disclaimers that apply to the journal pertain.

osteoblasts, a process termed bone remodeling.¹ Osteoclasts are derived from the monocyte cell lineage, that also gives rise to macrophages and dendritic cells. Monocytes and macrophages also function in bacterial and nanoparticle trapping and clearance.^{2, 3} Osteoclast differentiation is defined by an initial expression of tartrate resistant acid phosphatase (TRAP) by pre-osteoclasts following exposure to the key osteoclastogenic cytokine RANK ligand (RANKL) which leads to fusion with other pre-osteoclasts into multinucleated mature bone-resorbing osteoclasts.⁴ By contrast, osteoblasts are derived from bone marrow stromal cells, pluripotent progeny of mesenchymal stem cells and are defined by their capacity to deposit and mineralize collagen matrix as well as by tissue specific gene expression.⁵ Osteoblasts are characterized by their expression of key genes, coordinated in large measure through the key transcription factors Runx2^{5, 6} and Osterix⁷, involved in matrix production and mineral deposition including alkaline phosphatase, type I collagen, osteocalcin, osteopontin, and bone sialoprotein osteoblastic gene program. Factors that destabilize bone remodeling such as aging and inflammatory conditions including rheumatoid arthritis, bacterial and viral infections such as periodontitis⁸ and HIV-1⁹, and estrogen deficiency (associated with the menopause)¹⁰, lead to bone loss and dramatically increased risk of bone fractures.¹⁰

Although historically considered biocompatible but inert, studies have suggested a beneficial effect of dietary silica on skeletal development in rats¹¹, while clinical studies have reported strong positive associations between dietary silica intake and BMD in human cohorts.¹² Recently, silica has been incorporated into hydroxyapatite/bioceramic artificial bone scaffolds, where it is reported to enhance osteoconductivity.¹³⁻¹⁵ Silica is presumed to be non-toxic *in vivo* with concentrations as high as 50,000 ppm producing no adverse effects in rats.¹⁶ However, the mechanisms by which silica regulates skeletal development and function are presently unknown. The advent of nanotechnology has provided new opportunities to package and deliver bulk forms of certain elements with the nanoscale potentially enhancing biological processes. We postulated that silica in the form of nanoparticles would be bioactive and beneficial to the skeleton.

In this study we examined the effect of specific engineered 50 nm fluorescent silica based nanoparticles on the differentiation of osteoclasts and osteoblasts *in vitro* and on bone accretion *in vivo*. Results revealed that our nanoparticles possess strong biological activities including the suppression of osteoclast differentiation as well as the stimulation of osteoblast differentiation and mineralization *in vitro*. Additionally, our studies suggest that at least one mechanism by which the nanoparticles accomplish these disparate activities is by antagonizing the activation of the NF- κ B transcription factor, a signal transduction pathway that is potently inhibitory to osteoblast differentiation, but is essential for osteoclastogenesis. Finally, we show that *in vivo* silica nanoparticles have the capacity to enhance bone mineral density (BMD) in mice, suggesting their potential application as anti-osteoporotic agents.

Methods

Studies involving human tissues were conducted with informed consent and approval by the IRB. Animal studies were approved by the Emory IACUC and procedures followed in accordance with institutional guidelines for the humane care of the animals.

Materials

DMEM, EMEM, antibiotics (penicillin and streptomycin), and L-glutamine were purchased from Invitrogen Corp. (Carlsbad, CA) and α -MEM from (Irvine Scientific, Santa Ana, CA). FBS was from Atlanta Biologicals (Lawrenceville, GA). RANKL, TNF α , and M-CSF were

from R&D Systems (Minneapolis, MN). All other reagents were purchased from the Sigma Chemical Corporation, (St. Louis, MO) unless otherwise specified.

Nanoparticles

In this study, we utilized a specific 50 nm engineered silica nanoparticle formulation, referred to herein as NP1. NP1 comprises a solid silica shell (SiO₂) doped with the fluorescent dye rhodamine B (RhB). For *in vivo* experiments a magnetic nanoparticle (MNP) variant of NP1 containing an electron dense cobalt ferrite (CoFe₂O₄) core (NP1-MNP), and a polyethylene glycol (PEG) surface modification (NP1-MNP-PEG) was synthesized. The synthesis and characterization of all nanoparticles used in this study have been previously described in detail¹⁷⁻¹⁹ and the size distribution and Zeta potential are shown in Supplementary Figure 1.

Cell Culture

The pre-osteoblastic cell line MC3T3-E1 (MC3T3) was provided by Roland Baron (Yale University, New Haven, CT) and cultured in α -MEM + 10% FBS. The murine monocytic cell line RAW264.7 and the fibroblastic cell line NIH3T3 were purchased from the American Type Culture Collection (Manassas, VA) and cultured in DMEM + 10% FBS. The murine epidermal cell line JB6 (clone 41) was provided by Nancy Colburn (NCI, Frederick, MD) and cultured in EMEM + 4% FBS. All cultures contained 50 U/ml penicillin, 50 μ g/ml streptomycin and 2 mM L-glutamine and were grown at 37 °C and 5% CO₂.

Osteoclastogenesis assays

Osteoclasts were generated in 96 well plates using the monocytic cell line RAW264.7 as previously described.²⁰ Primary monocytes additionally received 25 ng/mL of the monocytic survival factor M-CSF. Cultures were treated with NP1 as indicated and after 7–10 days, cultures were stained for TRAP and the number of mature osteoclasts (TRAP positive with ≥ 3 nuclei) were counted under light microscopy and normalized for size. Each data point was performed in quadruplicate and data averaged.

Osteoblast differentiation and mineralization assays

MC3T3 cells or primary bone marrow stromal cells were purified as previously described²¹ and were plated at confluence in 24 or 96-well plates and differentiated to osteoblasts in differentiation medium (α -MEM supplemented with 10% FBS and 50 μ g L-ascorbate and, 10 mM β -glycerophosphate). Mineralization was visualized by fixing cells in 75% ethanol for 30 minutes at 4° C followed by staining with Alizarin Red-S (40 mM) for 10 minutes. Excess stain was removed by copious washing with distilled water.

Densitometry

Mineralization was quantified by scanning tissue culture plates at high resolution (2400 DPI) using a flatbed Epson Perfection 1660 photo scanner and densitometry performed using Image J Version 1.40g software.²²

Isolation of primary bone marrow stromal cells and monocytes

Female C57BL6 mice 6 weeks of age were purchased from Jackson Laboratories (Bar Harbor, Main). Mice were used to isolate bone marrow stromal cells for *in vitro* osteoblastic differentiation and mineralization assays as previously described²¹, or for splenic monocytes for osteoclast cultures as previously described.²³

Nanoparticle administration to mice *in vivo* and bone densitometry

For *in vivo* studies female C57BL6 mice, 9 wks of age, were injected intraperitoneally with NP1-MNP-PEG (50 mg/Kg) or with vehicle (phosphate buffered saline (PBS)), once per week for 6 weeks. Bone Mineral Density (BMD) analysis by Dual- Energy X-Ray Absorptiometry (DXA) was performed on a PIXImus2 bone densitometer (GE Medical Systems, Waukesha, WI) as previously described.²¹

NF- κ B, Wnt and Smad reporter constructs and luciferase assays

MC3T3 and RAW264.7 cells were transfected with the NF- κ B responsive reporter pNF κ B-LUC (BD Biosciences, San Jose, CA), the Smad reporter pGL3-Smad²¹ or the Wnt-responsive reporter TOPFLASH or its negative control FOPFLASH (Invitrogen), using Lipofectamine 2000 (Invitrogen). Transfection efficiency was verified in replicate cultures using pRL-SV40. The presence of nanoparticles in culture was confirmed to have no effect on transfection efficiency. Luciferase activity was measured on a microplate luminometer (Turner Designs, Sunnyvale, CA) using the luciferase assay system of Promega Corporation (Madison, WI) with passive lysis buffer. Data are expressed as Relative Light Units (RLU).

Electrophoretic mobility shift assay

MC3T3 cells were treated with TNF α (10 ng/mL) and NP1 nanoparticles (50 ng/mL) for 24 or 48 hr to assess the effect of NP1 exposure on long term NF- κ B expression. Nuclear and cytoplasmic fractions were isolated and incubated with the NF- κ B consensus oligonucleotide (Santa Cruz Biotechnology, Santa Cruz, CA) radiolabeled according to manufacturer's protocol (Promega) and reaction performed as described previously.²⁴

Statistical Analyses

Statistical significance was determined using GraphPad InStat version 3 for Windows XP (GraphPad Software). Multiple comparisons were performed by one-way ANOVA with Tukey-Kramer post-test or repeated measures ANOVA with Bonferroni multiple comparisons test. $p \leq 0.05$ was considered significant. (*) $p < 0.05$; (**) $p < 0.01$; (***) $p < 0.001$.

Results

Silica nanoparticles are stage specific inhibitors of osteoclastogenesis *in vitro*

Although dietary silica has long been held to be biocompatible and has been positively associated with bone health, the effects of silica in nanoparticle form have not been intensively studied, and their effects on bone metabolism are unknown. A significant proportion of the dietary silica that is absorbed into the circulation becomes resident in the skeleton. Furthermore, osteoclast precursors (monocytes) are involved in nanoparticle clearance and are consequently likely to encounter nanomaterials at high frequency *in vivo*. The response of monocytes to internalized silica nanoparticles and the effect(s) of nanosilica on bone cells such as osteoclasts and osteoblasts are presently unknown.

To examine the effect of silica nanoparticles on the differentiation of monocytes into osteoclasts we stimulated the mouse monocytic cell line RAW264.7 (an immortalized murine macrophage cell line) with the key osteoclastogenic cytokine RANKL (25 ng/mL) in the presence or absence of NP1, 50 nm silica nanoparticles in the concentration range 25 to 100 μ g/mL. Cultures were stained for the osteoclast marker TRAP (pink/purple cells) and photographed under light microscopy 7 days later (Figure 1A). RANKL alone stimulated the formation of large numbers of mononucleated TRAP⁺ preosteoclasts (small pink/red cells) that fused into giant multinucleated TRAP⁺ mature osteoclasts (large red/pink cells). Mature

multinucleated (≥ 3 nuclei by convention) TRAP⁺ osteoclasts were quantitated by counting under light microscopy with normalization for cell size (Figure 1B). NP1 significantly and dose-dependently reduced both osteoclast and TRAP⁺ pre-osteoclast formation.

To verify the capacity of NP1 to suppress osteoclastogenesis from primary monocytes, osteoclasts were cultured from purified mouse monocytes, treated with RANKL and the monocyte survival factor M-CSF (25 ng/mL), in the presence or absence of a range of NP1 concentrations. As with the RAW264.7 cells NP1 dose dependently suppressed primary monocyte differentiation into osteoclasts (Figure 1C). We further confirmed the ability of NP1 to suppress osteoclastogenesis using osteoclast precursors derived from human peripheral blood mononuclear cells (Supplementary Figure 2).

Osteoclasts form by fusion of TRAP⁺ mononucleated preosteoclasts into multinucleated mature osteoclasts. To examine the specific stage at which NP1 suppresses osteoclast formation we induced differentiation of RAW264.7 cells into osteoclasts using RANKL. NP1 was added at day 1, 3, or 5 of the 7 day culture and osteoclasts quantitated following TRAP staining (Figure 1D). NP1 specifically suppress early differentiation of osteoclast precursors into TRAP⁺ preosteoclasts (days 1–3), rather than the later fusion steps which occur around days 5 and 7 of culture.

NP1-MNP-PEG is a common multifunctional variant of NP1 comprising a CoFe₂O₄ magnetic metal core especially suitable for electron microscopic analysis, immunomagnetic isolation, and MRI imaging studies; and a polyethylene glycol (PEG) modified surface that allows enhanced *in vivo* biocompatibility and half-life. To assess whether these modifications have any effect on the anti-osteoclastogenic activity of the basal NP1 silica nanoparticle, RAW264.7 cells were induced to differentiate into osteoclasts in the presence of NP1-MNP-PEG. The results revealed that despite the internal core, and surface modification by PEG, the silica nanoparticles retained potent suppressive activity towards osteoclast formation (Figure 1E).

Interestingly, our data show that in nanoparticle form silica is not inert and in fact mediates potent anti-osteoclastogenic activities on monocytes by specifically blocking the differentiation of osteoclast precursors into TRAP⁺ pre-osteoclasts.

Silica nanoparticles do not mediate direct toxic effects or promote apoptosis of osteoclast precursors *in vitro*

Our data above demonstrated that silica nanoparticles suppress osteoclast differentiation *in vitro*. To determine whether these agents induce apoptosis of osteoclast precursors, RAW264.7 cells were treated with NP1 or vehicle for 7 days and apoptosis was examined by staining with Annexin V under fluorescence microscopy (Supplementary Figure 3A). No increase in basal apoptosis was observed with nanoparticle treated cultures, although significant nanoparticle incorporation was still apparent at 7 days of culture as observed by rhodamine B fluorescence associated with the nanoparticles (right lower panel). Cell viability assays (XTT) demonstrated that a dose range (10–100 $\mu\text{g/ml}$) of NP1 for up to 10 days failed to mediate any direct toxic effects on the viability or proliferation rates of RAW264.7 cells (Supplementary Figure 3B) suggesting that the anti-osteoclastogenic activities are related to suppression of differentiation along the osteoclast lineage, rather than a consequence of cell toxicity. NP1 also failed to impact the viability of JB6 epidermal cells, and NIH3T3 mouse fibroblasts (Supplementary Figure 3C and 3D). Furthermore, we have previously reported that NP1 does not impact the viability of MC3T3 osteoblast precursor cells, A549 human adenocarcinoma cells and HEK293 human embryonic kidney cells.¹⁷ Taken together these data suggest that NP1 is not inherently toxic to a wide range of cell

types, however possesses a capacity to antagonize the differentiation of osteoclast precursors into mature osteoclasts.

Silica nanoparticles are potent stimulators of osteoblast differentiation and mineralization in vitro

The osteoblast precursor cell line MC3T3^{25, 26} have been used extensively by us^{21, 27–29} and others to study multiple aspects of osteoblast differentiation and activity²⁶ and to populate artificial mineralized nanofiber scaffolds for use in tendon-to-bone tissue repair.³⁰ MC3T3 cells are also known to readily internalize silica nanoparticles.¹⁷ We thus used these cells to examine the effect of NP1 on osteoblast differentiation and activity. MC3T3 cells were cultured in osteogenic medium containing L-ascorbate (50 µg/mL) and 10 mM β-glycerophosphate to promote differentiation into the osteoblast lineage²¹ in the presence of a range of NP1 concentrations. In osteogenic medium MC3T3 cells typically differentiate into mineralizing osteoblasts over a period of 21 days. Surprisingly, mineralization nodules were readily detectable following Alizarin Red-S staining for calcium deposition after only 10 days of culture in the presence of NP1 (Figure 2A). NP1 further enhanced the *ex vivo* differentiation and mineralization of primary mouse bone marrow stromal cells over 21 days of culture (Figure 2B). We further ratified that NP1-MNP-PEG was also capable of accelerating the differentiation of MC3T3 cells into mineralizing osteoblasts (Figure 2C) demonstrating that surface and core modifications did not impact the biological activity of this nanomaterial on osteoblasts. NP1 further stimulate mineralization by osteoclasts differentiated from human bone marrow stromal cells (Supplementary Figure 4).

To determine whether silica nanoparticles enhance osteoblast function (mineralization) directly or act by promoting osteoblast differentiation we examined the expression of characteristic osteoblast genes by northern blot. NP1 dose-dependently upregulated the expression of key osteoblast matrix proteins including bone sialoprotein, osteocalcin, and osteopontin by 7 days of culture. Furthermore, the nanoparticles stimulated expression of Osterix, a key transcription factor involved in osteoblast differentiation (Figure 3A).

Like Osterix, Runx2 is a transcription factor known to be essential for osteoblastic differentiation. NP1 potently upregulated Runx2 while tumor necrosis factor alpha (TNFα), a known inhibitor of osteoblast differentiation and of Runx2 expression^{21, 31}, as expected suppressed Runx2 induction (Figure 3B). NP1 exhibited no significant effects on osteoblastic gene induction in non-osteoblastic cell lines including RAW264.7 and NIH3T3, demonstrating cell specific activity (Figure 3C). These data suggest that NP1 likely induces osteoblastic gene products by promoting the differentiation of preosteoblasts towards the osteoblast lineage, rather than by directly acting on osteoblastic gene promoters.

Silica nanoparticles do not stimulate or chelate reactive oxygen species (ROS)

Silica nanoparticles have been reported to mediate pro-inflammatory responses as a consequence of the generation of reactive oxygen species (ROS) in macrophages and RAW264.7 cells, leading to potential toxic effects and diminished cell proliferation.³² In contrast, other nanoparticle formulations are reported to scavenge ROS.³³ ROS have been reported to be potent stimulators of osteoclastogenesis *in vivo*³⁴ and are associated with osteoblast and osteocyte apoptosis.³⁵ To investigate whether the effects of NP1 on osteoblast and osteoclast differentiation are mediated by induction of, or scavenging ROS we treated MC3T3 cells and RAW264.7 cells (Supplementary Figures 5 A and 5B respectively) with NP1 (50 µg/mL) for 1 hr then loaded cells with the fluorescent indicator of ROS. NP1 neither generated ROS nor sequestered ROS in these experiments. Taken together, our data suggest that ROS and changes in cell proliferation are not the pertinent

mechanism by which NP1 stimulates osteoblast differentiation and/or suppresses osteoclast differentiation.

Silica nanoparticles do not stimulate a general inflammatory response

Previous studies have suggested that cell exposure to silica, in particular crystalline silica in alveolar macrophages of the lung, initiates an inflammatory response characterized by induction of IL-1 β (reviewed in³⁶). To determine if our 50 nm spherical nanoparticles stimulate an inflammatory response RAW264.7 cells were treated with NP1, or NP1-PEG a variant conjugated with polyethylene glycol (PEG). Relative to untreated control neither NP1 nor NP1-PEG had any significant effect on the inflammasome based cleavage of the 38 kDa IL-1 β precursor into its active 17 kDa species. By contrast, 2 μ g/ml lipopolysaccharide (LPS) a known activator of IL-1 transcription and the inflammasome, enhanced production of both IL-1 precursor and cleavage into its processed form (Supplemental Figure 6A and 6B). RT-PCR analysis further revealed that LPS promoted IL-1 β transcription while nanoparticles had no effect (Supplemental Figure 6C).

Silica nanoparticles suppress NF- κ B activation in osteoclasts and osteoblasts

We have previously reported that several compounds possessing the unusual property of differentially regulating osteoclast and osteoblast formation and activity achieve these actions by modulating the NF- κ B signal transduction pathway.^{20, 28, 29, 37–39} The NF- κ B transcription factor is well known to be critical for osteoclast differentiation⁴⁰, yet is potently inhibitory to osteoblast differentiation and activity.^{21, 41} Consequently, antagonists of NF- κ B promote osteoblast differentiation but suppress osteoclast formation.^{20, 28, 29, 37–39} This provided us with a clue as to the potential mechanism of silica nanoparticle activity.

To determine whether silica nanoparticles promote osteoblastogenesis and suppress osteoclastogenesis by inhibiting NF- κ B activation we transfected MC3T3 and RAW264.7 cells with a luciferase reporter driven by tandem NF- κ B consensus motifs²¹ and treated the cells with silica nanoparticles. Luciferase activity was read 24 hr later and NP1 was found to dose-dependently suppress basal (Figure 4A) and RANKL-induced NF- κ B transactivation in RAW264.7 cells (Figure 4B). NP1 further inhibited TNF α -induced NF- κ B transactivation activity in MC3T3 cells (Figure 4C). Interestingly, we found that NP1 did not repress TNF α -induced NF- κ B reporter activity in HEK293 cells (Figure 4D), a TNF α responsive cell line, suggesting some degree of cell type specificity of action.

We further validated the capacity of NP1 to chronically suppress NF- κ B signaling in MC3T3 cells. Although TNF α induced significant gel retardation of an oligonucleotide containing a NF- κ B consensus sequence at 24 and 48 hr after exposure of MC3T3 cells as demonstrated by EMSA, NP1 potently diminished NF- κ B binding to its consensus binding site (Figure 5A). As the NF- κ B subunits p50 and p52 have been demonstrated to be critical to osteoclast differentiation^{42–44} while p50 has been implicated in downregulation of osteoblastic genes⁴¹ we used Western blotting to examine the effect of NP1 on p50 and p52. NP1 was found to suppress the TNF α -induced proteolytic cleavage of p105 into active p50 NF- κ B subunits in MC3T3 cells (Figure 5B). Furthermore, NP1 suppressed the RANKL-induced translocation of p52 NF- κ B subunits from cytosol (Figure 5C) to nucleus (Figure 5D) in RAW264.7 cells.

Silica nanoparticles fail to regulate Smad or Wnt expression in osteoblasts

Smad signal transduction induced by TGF β or BMPs is well established to promote osteoblast commitment and differentiation, as is activation of the β -catenin transcription factor downstream of the Wnt signal transduction pathway. We consequently also examined

the effect of silica nanoparticles on these pathways using Smad and Wnt responsive luciferase reporter constructs. NP1 failed to modulate either a Smad-responsive luciferase reporter transactivated by all Smad heterodimers²¹ (Supplementary Figure 7A) or the β -catenin responsive TCF-reporter construct pTOPFLASH in MC3T3 cells (Supplementary Figure 7B) demonstrating a considerable degree of specificity.

Silica nanoparticles enhance bone mineral density in mice *in vivo*

As silica nanoparticles stimulated osteoblast differentiation and mineralization and inhibited osteoclast differentiation *in vitro*, we examined the capacity of our nanoparticles to enhance BMD in mice. NP1-MNP-PEG, a surface modified NP1-MNP variant containing PEG groups that are reported to enhance biocompatibility and *in vivo* half-life^{17, 19}, were injected intraperitoneally into mice 9 weeks of age, weekly for 6 weeks. BMD was followed prospectively at baseline (0) and at 2, 4, and 6 weeks of treatment. Our data show a statistically significant increase in BMD at the lumbar spine, within 2 weeks of treatment (Figure 6A) while the increase in femoral BMD reached statistical significance by 6 weeks of treatment (Figure 6B).

Discussion

Although dietary silica has long been held to be biocompatible and has been positively associated with bone health, the effects of silica in nanoparticle form have not been investigated in relation to bone metabolism. Osteoclast precursors (monocytes) are involved in nanoparticle clearance and are consequently likely to encounter nanomaterials at high frequency *in vivo*. Furthermore, a significant proportion of the dietary silica that is absorbed into the circulation becomes resident in the skeleton. The response of monocytes to internalized silica nanoparticles and the effect(s) of nanosilica on bone cells such as osteoclasts and osteoblasts are unknown and were the focus of this study. Interestingly, our data show that in nanoparticle form silica is not inert and in fact mediates potent anti-osteoclastogenic activities on monocytes. These activities were not associated with direct toxicity as neither apoptosis nor viability was impacted. Rather, silica nanoparticles were found to specifically block the differentiation of osteoclast precursors into TRAP+ pre-osteoclasts.

In contrast to the inhibitory effects on osteoclast differentiation, the silica nanoparticles stimulated the mineralization of differentiating of osteoblast precursors. Previous reports have indicated that mesoporous silica nanoparticles have no effect on viability, proliferation, immunophenotype, or differentiation of mesenchymal stem cells (osteoblast precursors) *in vitro*.⁴⁵ We similarly did not identify inhibitory effects on cell viability or proliferation rate, however, our data differ from this study in terms of differentiation of osteoblast precursors and reveal potent osteoblastogenic activity of silica nanoparticles. One key factor that may explain the difference in response is the 50 nm size of the nanoparticles utilized in our studies as compared to the 110 nm nanoparticles used in the previous study. Another key difference is shape; while we utilized spherical silica nanoparticles the silica nanoparticles utilized by Huang et al. were hexagonal. These data suggest that subtle changes in charge, shape, size, and/or surface chemistry may lead to very different physicochemical properties of silica nanoparticles in biological systems. Interestingly, addition of a PEG surface decoration to our silica nanoparticles did not mask their biological activities on bone cells.

We have previously reported that several compounds possessing the unusual property of differentially regulating osteoclast and osteoblast formation and activity achieve these actions by modulating the NF- κ B signal transduction pathway.^{20, 28, 29, 37–39} This provided us with a clue as to the potential mechanism of silica nanoparticle activity and, consistent with our previous reports, silica nanoparticles were indeed found to suppress NF- κ B

activation in osteoclasts and osteoblasts, providing a basis and molecular mechanism to explain their action. How NP1 modulates NF- κ B activity is presently unknown and may involve direct interactions with key activators or inhibitors of the NF- κ B system, indirect actions of the transcription of NF- κ B transcription factors or their regulators, or through modulation of NF- κ B and or I κ B processing via the proteasome. These potential mechanisms remain to be investigated.

The ability of NP1 to suppress TNF α -induced NF- κ B transactivation activity in osteoblast precursors has important implications for silica nanoparticle action *in vivo*. We have reported that TNF α is a potent *in vivo* suppressor of bone formation as TNF α and its Type I receptor knockout mice have significantly enhanced BMD as a consequence of dramatically elevated bone formation.²¹ By contrast TNF α is well established to promote osteoclastic bone destruction in multiple inflammatory conditions including postmenopausal osteoporosis and rheumatoid arthritis. Suppression of NF- κ B signal transduction by TNF α may thus have potent anabolic and anticatabolic activities on the skeleton *in vivo*. In fact, our data show that NP1-MNP-PEG does indeed promote bone accesion in mice *in vivo*.

In the context of normal bone remodeling our *in vitro* and *in vivo* results suggest that NP1 is capable of altering cell behavior through specific cellular and molecular mechanisms. It is therefore expected that the particles would act directly on the cells responsible for bone remodeling. However, it remains to be determined how the particles achieve localization to bone. Because the bone microenvironment is highly vascularized nanoparticles are likely deposited near bone cells and have the potential to enter osteoclasts and osteoblasts and/or their precursors directly promoting bone formation and decreasing resorptive activity. However, osteoclast precursors are ubiquitous in the body and are likely exposed to nanoparticles not only in the bone microenvironment but also in the peripheral circulation and in lymphoid and other tissues where they serve immune-related functions and actively phagocytose nanomaterials.^{2, 3} Furthermore, nanoparticles may become intercalated into the bone matrix and or deposited on bone surfaces by osteoblasts during matrix synthesis and mineralization. Thus far we have not been successful in visualizing nanoparticles incorporated into mouse bone *in vivo* using fluorescence. However, because bone has strong auto-fluorescence in the same wavelength as rhodamine B, we cannot exclude the possibility that a low concentration of nanoparticles have been incorporated into bone, given that the doses we use are likely inadequate to effectively coat bone surfaces to any degree. Should nanoparticles indeed incorporate into bone they may be further released during osteoclastic bone resorption and dampen osteoclast activity in a manner analogous to that of the bisphosphonate class of anti-resorptive drugs that associate with hydroxyapatite and are released by osteoclasts during resorption leading to osteoclast apoptosis.

Hydroxyapatite is itself recognized to be an osteoconductive material and hydroxyapatite coatings are ideal surfaces for the function of osteoblasts⁴⁶. It is unlikely however that these pro-osteoblastic actions are mediated though NF- κ B suppression given that hydroxyapatite also affords good biodegradability to osteoclasts⁴⁶ which attach to and resorb hydroxyapatite with alacrity.

In conclusion, our data show that 50 nm silica-based nanoparticles stimulate osteoblast differentiation and mineralization and suppress osteoclast differentiation *in vitro*, while enhancing peak BMD *in vivo*. Bioactive silica-based nanoparticles may consequently have significant potential for use as novel dual anabolic and anticatabolic pharmaceuticals for increasing basal BMD and/or for the amelioration of bone diseases for fracture prevention. Furthermore, to our knowledge, this is the first example of a nanoparticle formulation having intrinsic net beneficial bioactivities on an organ system and promotes the concept

that nanoparticles may be endowed with inherent biological activities exploitable for disease amelioration has yet to be reported.

Supplementary Material

Refer to Web version on PubMed Central for supplementary material.

Acknowledgments

This study was supported by a grant from NIAMS (AR056090) and by a Georgia Research Alliance grant (GRA.VL12.C2) to M.N. Weitzmann and G.R. Beck. M.N. Weitzmann is also supported in part by funding from the Biomedical Laboratory Research & Development Service of the VA Office of Research and Development (5I01BX000105) and by grants AR059364 and AR053607 from NIAMS and AG040013 from NIA. G.R. Beck is also supported in part by NCI grants (CA136059 and CA136716). J-K. Lee expresses his thanks for a fellowship from the SBS Foundation in Korea to initiate this research collaboration.

References

1. Riggs BL, Khosla S, Melton LJ 3rd. Sex steroids and the construction and conservation of the adult skeleton. *Endocr Rev.* 2002; 23:279–302. [PubMed: 12050121]
2. Cho M, Cho WS, Choi M, Kim SJ, Han BS, Kim SH, et al. The impact of size on tissue distribution and elimination by single intravenous injection of silica nanoparticles. *Toxicol Lett.* 2009; 189:177–183. [PubMed: 19397964]
3. Bartneck M, Keul HA, Zwadlo-Klarwasser G, Groll J. Phagocytosis independent extracellular nanoparticle clearance by human immune cells. *Nano Lett.* 2010; 10:59–63. [PubMed: 19994869]
4. Teitelbaum SL. Bone resorption by osteoclasts. *Science.* 2000; 289:1504–1508. [PubMed: 10968780]
5. Ducy P, Zhang R, Geoffroy V, Ridall AL, Karsenty G. *Osf2/Cbfa1*: a transcriptional activator of osteoblast differentiation. *Cell.* 1997; 89:747–754. [PubMed: 9182762]
6. Lee KS, Kim HJ, Li QL, Chi XZ, Ueta C, Komori T, et al. *Runx2* is a common target of transforming growth factor beta1 and bone morphogenetic protein 2, and cooperation between *Runx2* and *Smad5* induces osteoblast-specific gene expression in the pluripotent mesenchymal precursor cell line C2C12. *Mol Cell Biol.* 2000; 20:8783–8792. [PubMed: 11073979]
7. Nakashima K, Zhou X, Kunkel G, Zhang Z, Deng JM, Behringer RR, et al. The novel zinc finger-containing transcription factor osterix is required for osteoblast differentiation and bone formation. *Cell.* 2002; 108:17–29. [PubMed: 11792318]
8. Wactawski-Wende J. Periodontal diseases and osteoporosis: association and mechanisms. *Annals of periodontology / the American Academy of Periodontology.* 2001; 6:197–208. [PubMed: 11887465]
9. Vikulina T, Fan X, Yamaguchi M, Roser-Page S, Zayzafoon M, Guidot DM, et al. Alterations in the immuno-skeletal interface drive bone destruction in HIV-1 transgenic rats. *Proc Natl Acad Sci U S A.* 2010; 107:13848–13853. [PubMed: 20643942]
10. Weitzmann MN, Pacifici R. Estrogen deficiency and bone loss: an inflammatory tale. *J Clin Invest.* 2006; 116:1186–1194. [PubMed: 16670759]
11. Schwarz K, Milne DB. Growth-promoting effects of silicon in rats. *Nature.* 1972; 239:333–334. [PubMed: 12635226]
12. Jugdaohsingh R. Silicon and bone health. *J Nutr Health Aging.* 2007; 11:99–110. [PubMed: 17435952]
13. Gibson IR, Best SM, Bonfield W. Chemical characterization of silicon-substituted hydroxyapatite. *J Biomed Mater Res.* 1999; 44:422–428. [PubMed: 10397946]
14. Keeting PE, Oursler MJ, Wiegand KE, Bonde SK, Spelsberg TC, Riggs BL. Zeolite A increases proliferation, differentiation, and transforming growth factor beta production in normal adult human osteoblast-like cells *in vitro*. *J Bone Miner Res.* 1992; 7:1281–1289. [PubMed: 1334616]

15. Zou S, Ireland D, Brooks RA, Rushton N, Best S. The effects of silicate ions on human osteoblast adhesion, proliferation, and differentiation. *Journal of biomedical materials research*. 2009; 90:123–130. [PubMed: 19194862]
16. Martin KR. The Chemistry of Silica and its Potential Health Benefits. *J Nutr Health Aging*. 2007; 11:94–97. [PubMed: 17435951]
17. Ha SW, Camalier CE, Beck GR Jr, Lee J-K. New method to prepare very stable and biocompatible fluorescent silica nanoparticles. *Chem Commun (Camb)*. 2009:2881–2883. [PubMed: 19436897]
18. Kim JS, Yoon TJ, Yu KN, Noh MS, Woo M, Kim BG, et al. Cellular uptake of magnetic nanoparticle is mediated through energy-dependent endocytosis in A549 cells. *J Vet Sci*. 2006; 7:321–326. [PubMed: 17106221]
19. Yoon TJ, Yu KY, Kim E, Kim JS, Kim BG, Yun S-H, et al. Specific Targeting, Cell Sorting, and Bioimaging with Smart Magnetic Silica Core-Shell Nanomaterials. *Small*. 2006; 2:209–215. [PubMed: 17193022]
20. Yamaguchi M, Weitzmann MN. Vitamin K2 stimulates osteoblastogenesis and suppresses osteoclastogenesis by suppressing NF-kappaB activation. *Int J Mol Med*. 2011; 27:3–14. [PubMed: 21072493]
21. Li Y, Li A, Strait K, Zhang H, Nanes MS, Weitzmann MN. Endogenous TNFalpha Lowers Maximum Peak Bone Mass and Inhibits Osteoblastic Smad Activation, through NF-kappaB. *J Bone Miner Res*. 2007; 22:646–655. [PubMed: 17266397]
22. Abramoff MD, Magelhaes PJ, Ram SJ. Image Processing with ImageJ. *Biophotonics International*. 2004; 11:36–42.
23. Toraldo G, Roggia C, Qian WP, Pacifici R, Weitzmann MN. IL-7 induces bone loss-*in vivo* by induction of receptor activator of nuclear factor kappa B ligand and tumor necrosis factor alpha from T cells. *Proc Natl Acad Sci U S A*. 2003; 100:125–130. [PubMed: 12490655]
24. Camalier CE, Young MR, Bobe G, Perella CM, Colburn NH, Beck GR Jr. Elevated phosphate activates N-ras and promotes cell transformation and skin tumorigenesis. *Cancer Prev Res (Phila)*. 2010; 3:359–370. [PubMed: 20145188]
25. Sudo H, Kodama HA, Amagai Y, Yamamoto S, Kasai S. *In vitro* differentiation and calcification in a new clonal osteogenic cell line derived from newborn mouse calvaria. *J Cell Biol*. 1983; 96:191–198. [PubMed: 6826647]
26. Wang D, Christensen K, Chawla K, Xiao G, Krebsbach PH, Franceschi RT. Isolation and characterization of MC3T3-E1 preosteoblast subclones with distinct *in vitro* and *in vivo* differentiation/mineralization potential. *J Bone Miner Res*. 1999; 14:893–903. [PubMed: 10352097]
27. Beck GR Jr, Sullivan EC, Moran E, Zerler B. Relationship between alkaline phosphatase levels, osteopontin expression, and mineralization in differentiating MC3T3-E1 osteoblasts. *J Cell Biochem*. 1998; 68:269–280. [PubMed: 9443082]
28. Yamaguchi M, Weitzmann MN. The estrogen 17beta-estradiol and phytoestrogen genistein mediate differential effects on osteoblastic NF-kappaB activity. *Int J Mol Med*. 2009; 23:297–301. [PubMed: 19148557]
29. Yamaguchi M, Weitzmann MN. The bone anabolic carotenoid beta-cryptoxanthin enhances transforming growth factor-beta1-induced SMAD activation in MC3T3 preosteoblasts. *Int J Mol Med*. 2009; 24:671–675. [PubMed: 19787201]
30. Li X, Xie J, Lipner J, Yuan X, Thomopoulos S, Xia Y. Nanofiber scaffolds with gradations in mineral content for mimicking the tendon-to-bone insertion site. *Nano Lett*. 2009; 9:2763–2768. [PubMed: 19537737]
31. Gilbert L, He X, Farmer P, Rubin J, Drissi H, van Wijnen AJ, et al. Expression of the osteoblast differentiation factor RUNX2 (Cbfa1/AML3/Pebp2alpha A) is inhibited by tumor necrosis factor-alpha. *J Biol Chem*. 2002; 277:2695–2701. [PubMed: 11723115]
32. Park EJ, Park K. Oxidative stress and pro-inflammatory responses induced by silica nanoparticles *in vivo* and *in vitro*. *Toxicol Lett*. 2009; 184:18–25. [PubMed: 19022359]
33. Hamasaki T, Kashiwagi T, Imada T, Nakamichi N, Aramaki S, Toh K, et al. Kinetic Analysis of Superoxide Anion Radical-Scavenging and Hydroxyl Radical-Scavenging Activities of Platinum Nanoparticles. *Langmuir*. 2008

34. Grassi F, Tell G, Robbie-Ryan M, Gao Y, Terauchi M, Yang X, et al. Oxidative stress causes bone loss in estrogen-deficient mice through enhanced bone marrow dendritic cell activation. *Proc Natl Acad Sci U S A*. 2007; 104:15087–15092. [PubMed: 17848519]
35. Almeida M, Han L, Martin-Millan M, Plotkin LI, Stewart SA, Roberson PK, et al. Skeletal involution by age-associated oxidative stress and its acceleration by loss of sex steroids. *J Biol Chem*. 2007; 282:27285–27297. [PubMed: 17623659]
36. Hamilton RF Jr, Thakur SA, Holian A. Silica binding and toxicity in alveolar macrophages. *Free Radic Biol Med*. 2008; 44:1246–1258. [PubMed: 18226603]
37. Yamaguchi M, Weitzmann MN. The bone anabolic carotenoids p-hydroxycinnamic acid and beta-cryptoxanthin antagonize NF-kappaB activation in MC3T3 preosteoblasts. *Mol Med Report*. 2009; 2:641–644. [PubMed: 21475879]
38. Yamaguchi M, Weitzmann MN. Zinc stimulates osteoblastogenesis and suppresses osteoclastogenesis by antagonizing NF-kappaB activation. *Molecular and cellular biochemistry*. 2011
39. Yamaguchi M, Weitzmann MN. Quercetin, a potent suppressor of NF-kappaB and Smad activation in osteoblasts. *International journal of molecular medicine*. 2011
40. Boyce BF, Yao Z, Xing L. Functions of nuclear factor kappaB in bone. *Ann N Y Acad Sci*. 2010; 1192:367–375. [PubMed: 20392262]
41. Nanes MS. Tumor necrosis factor-alpha: molecular and cellular mechanisms in skeletal pathology. *Gene*. 2003; 321:1–15. [PubMed: 14636987]
42. Xing L, Carlson L, Story B, Tai Z, Keng P, Siebenlist U, et al. Expression of either NF-kappaB p50 or p52 in osteoclast precursors is required for IL-1-induced bone resorption. *J Bone Miner Res*. 2003; 18:260–269. [PubMed: 12568403]
43. Novack DV, Yin L, Hagen-Stapleton A, Schreiber RD, Goeddel DV, Ross FP, et al. The IkappaB function of NF-kappaB2 p100 controls stimulated osteoclastogenesis. *J Exp Med*. 2003; 198:771–781. [PubMed: 12939342]
44. Boyce BF, Xing L, Franzoso G, Siebenlist U. Required and nonessential functions of nuclear factor-kappa B in bone cells. *Bone*. 1999; 25:137–139. [PubMed: 10423039]
45. Huang DM, Hung Y, Ko BS, Hsu SC, Chen WH, Chien CL, et al. Highly efficient cellular labeling of mesoporous nanoparticles in human mesenchymal stem cells: implication for stem cell tracking. *Faseb J*. 2005; 19:2014–2016. [PubMed: 16230334]
46. Hao J, Kuroda S, Ohya K, Bartakova S, Aoki H, Kasugai S. Enhanced osteoblast and osteoclast responses to a thin film sputtered hydroxyapatite coating. *J Mater Sci Mater Med*. 2011; 22:1489–1499. [PubMed: 21567286]

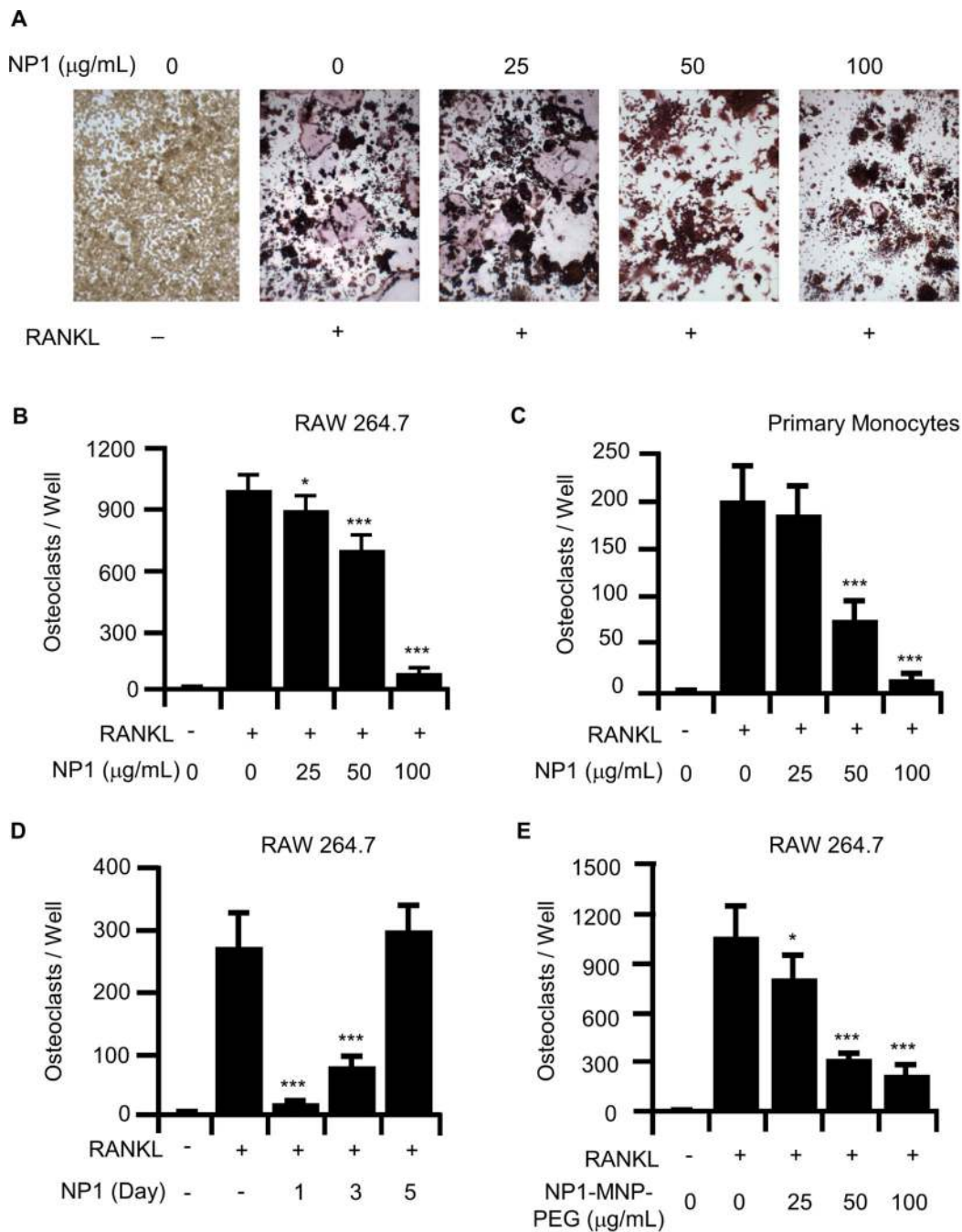


Figure 1.

Silica nanoparticles suppress osteoclastogenesis *in vitro*. (A) NP1 dose dependently inhibits RANKL (25 ng/mL) induced osteoclast formation. TRAP stained osteoclasts (pink) were photographed under light microscopy at 100X magnification. (B) Mature multinucleated (≥ 3 nuclei) TRAP osteoclasts were quantitated in NP1 treated RAW 264.7 cell cultures. (C) NP1 dose dependently inhibits differentiation of primary splenic mouse monocytes into osteoclasts cultured with RANKL (25 ng/mL) and M-CSF (25 ng/mL). (D) RAW264.7 cells were differentiated into osteoclasts with RANKL (25 ng/mL) and NP1 (50 $\mu\text{g/mL}$) added at day 1, 3, or 5 of culture. Cultures were TRAP stained at day 7 and mature osteoclast

quantitated. All data points represent Mean + SD of 4 replicate wells and are representative of 3 or more independent experiments. * $p < 0.05$, *** $p < 0.001$ relative to RANKL only. One-way ANOVA, Tukey-Kramer post test.

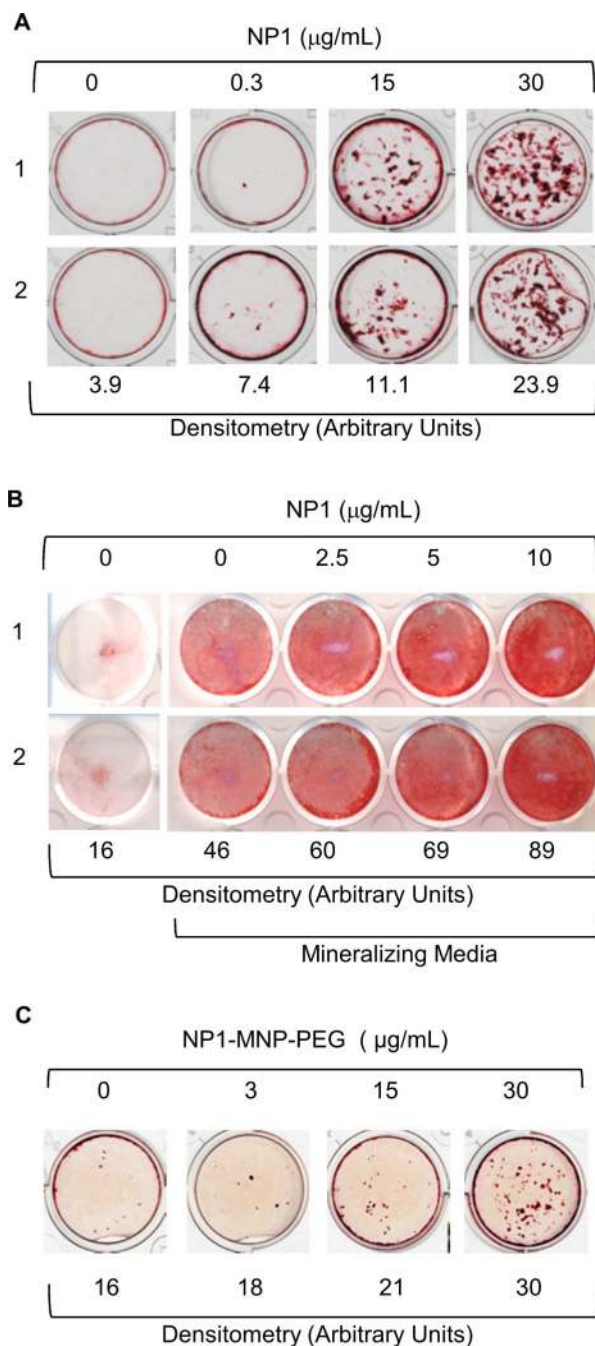


Figure 2.

NP1 nanoparticles stimulate osteoblast differentiation and mineralization *in vitro*. (A) NP1 dose-dependently induces mineralization nodules in MC3T3 cultures. Cultures were stained for calcium depositions by Alizarin Red-S at day 10. Mineralization was quantitated using Image J and averaged for each experiment (Densitometry). Two independent experiments are shown (labeled 1 and 2). (B) NP1 stimulates mineralization by primary mouse bone marrow stromal cells. Cultures were stained for calcium deposition by Alizarin Red-S at day 16. Independent experiments (labeled as 1 and 2) are shown and mineralization was quantitated using Image J and averaged for each experiment. (C) NP1-MNP-PEG was

assessed for osteoblast differentiation and mineralization activity at 10 days. Data representative of at least 3 independent experiments.

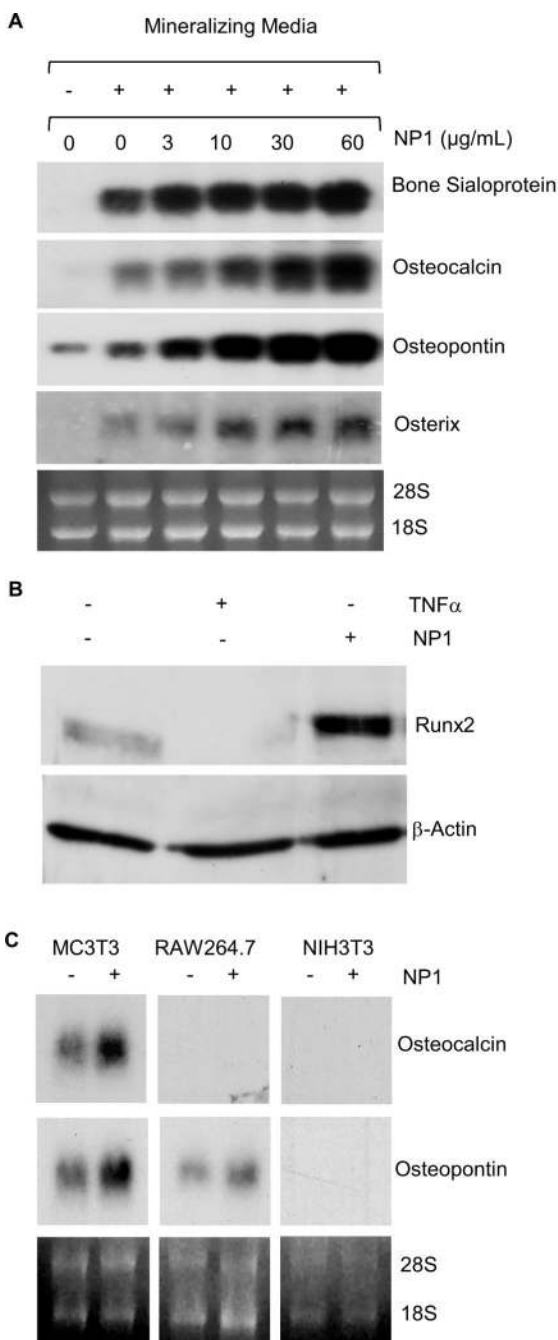


Figure 3.

Silica nanoparticles promote an osteoblastic gene differentiation program. (A) NP1 dose-dependently induces expression of the characteristic osteoblastic gene products bone sialoprotein, osteocalcin, and osteopontin in MC3T3 cells, quantitated by northern blot. (B) Western blot of NP1 (50 $\mu\text{g/mL}$ for 18 hr) stimulated expression of Runx2. TNF α (10 ng/ml), a known inhibitor of Runx2, was added as a control. (C) Osteocalcin and osteopontin are selectively upregulated by NP1 in pre-osteoblasts (Northern blot). Data representative of two independent experiments.

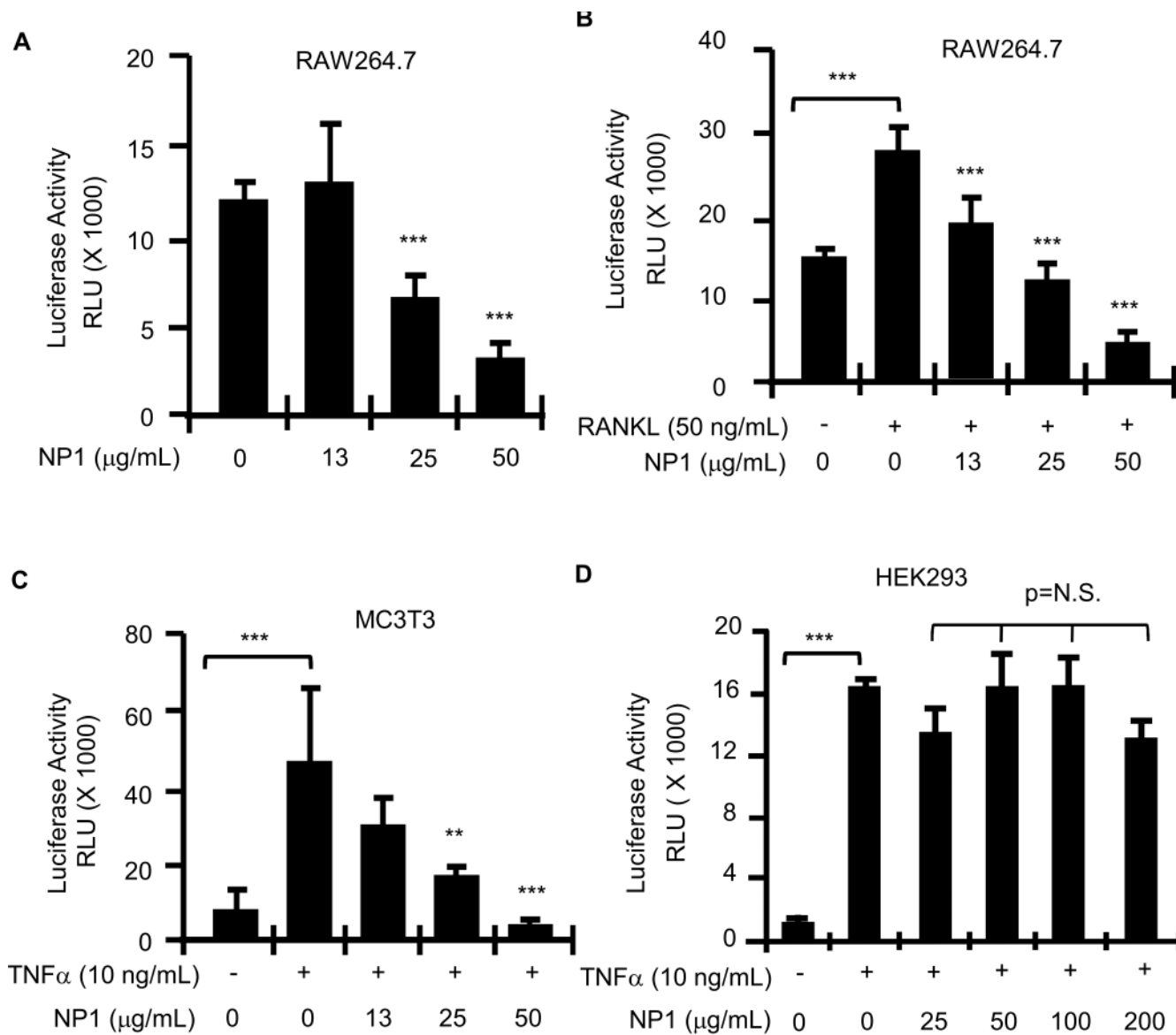


Figure 4. Silica Nanoparticles dose-dependently suppress NF- κ B activation in MC3T3 cells and RAW264.7 cells. NP1 dose-dependently suppresses basal (A) and (B) RANKL-induced NF- κ B activation in RAW264.7 cells, and (C) TNF α (10 ng/ml) induced NF- κ B activation in MC3T3 cells. Cell lines were transfected with an NF- κ B-responsive luciferase reporter and luciferase activity quantitated 24 hr later. Data expressed as Relative Light Units (RLU). (D) NP1 fails to suppress TNF α -induced NF- κ B in HEK293 cells. All data points represent the average + SD of 4 replicate wells and 3 or more independent experiments.

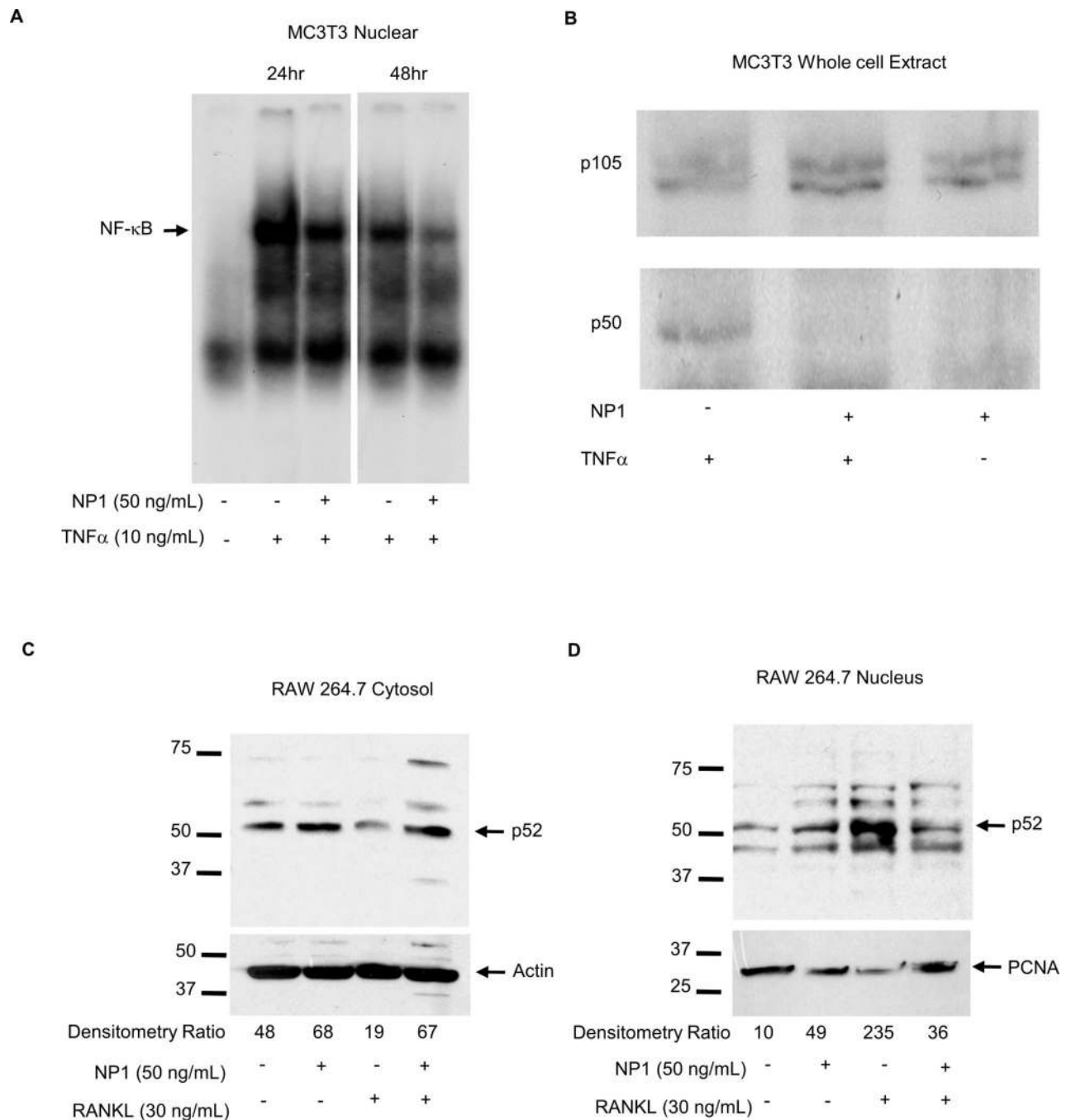


Figure 5.

Silica nanoparticles antagonize NF- κ B activation in osteoclast and osteoblast precursors. (A) MC3T3 cells were stimulated with TNF α (10 ng/mL) with or without NP1 (50 ng/mL) for 24 or 48 hr and nuclear extracts isolated for EMSA using radiolabeled NF- κ B consensus probe. (B) MC3T3 cells were treated with TNF α and/or NP1 for 24 hr and whole cell extracts isolated for western blots. Blots were immunoprobed for NF- κ B subunit p50 and its precursor p105. (C) RAW264.7 cells were treated with RANKL and/or NP1 for 24 hr and cytosolic and nuclear extracts isolated for Western blots. Blots were immunoprobed for NF- κ B subunit p52. Actin and PCNA antibodies were used as loading controls for cytosol and

nuclear extracts respectively. Densitometry scanning of bands and the actin/p52 or PCNA/p52 ratios are shown below the gels.

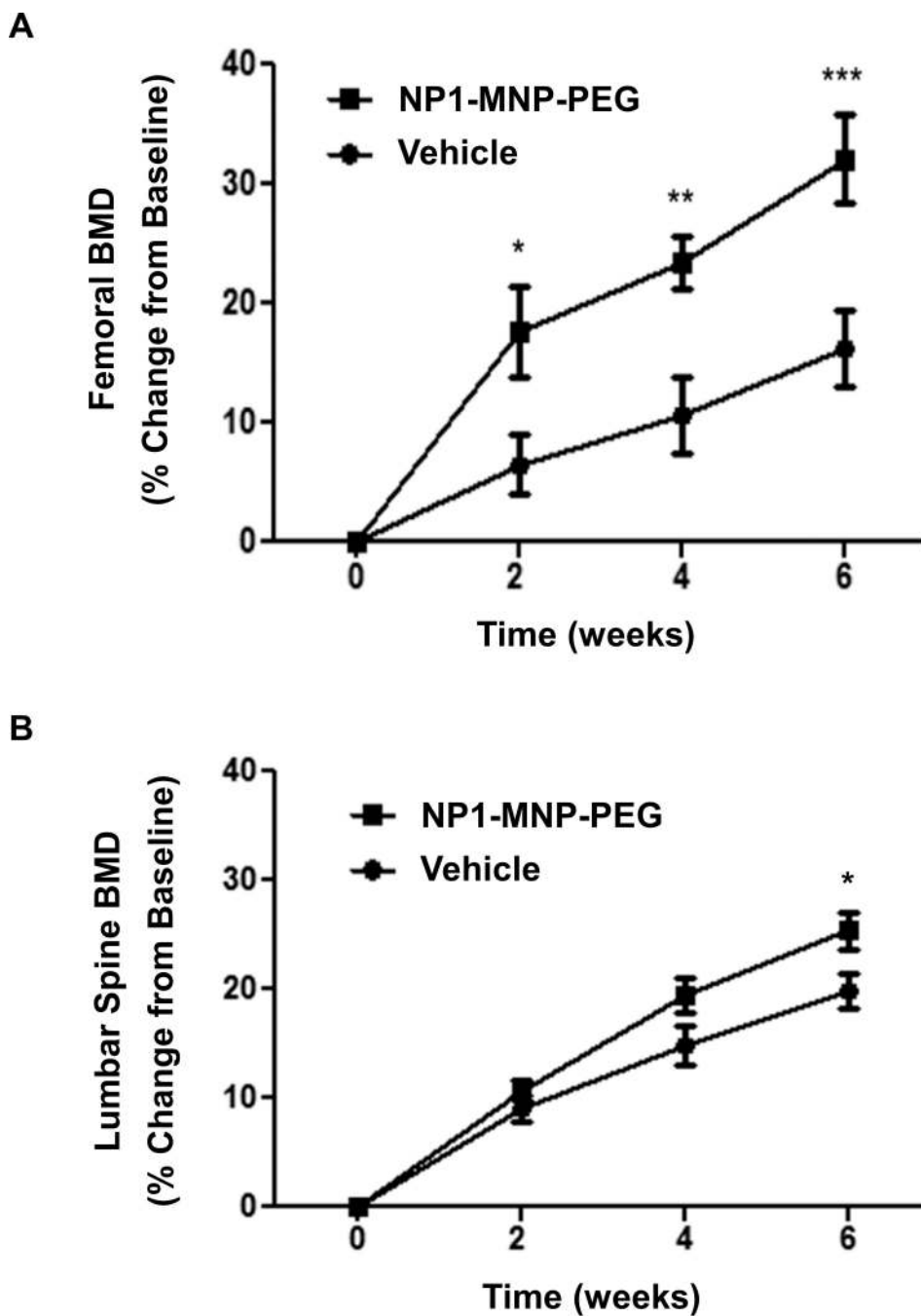


Figure 6. Silica nanoparticles enhance peak bone mineral density in mice *in vivo*. Female C57BL6 mice, 9 wks of age were injected intraperitoneally with NP1-MNP-PEG (50 mg/Kg) or vehicle, weekly for 6 weeks. BMD was quantitated at (A) the femur and (B) lumbar spine by DXA at baseline and at 2 week intervals up to 6 weeks and is presented as Mean \pm SEM of percentage change from baseline, calculated for each mouse. For femurs, left and right femurs were averaged for each independent mouse. N= 9 mice per group. * $p < 0.05$, ** $p < 0.01$ or *** $P < 0.001$ by repeated measures ANOVA with Bonferroni multiple comparisons test.